

# SCALING PROPERTIES OF THE ENERGY DENSITY IN SU(2) LATTICE GAUGE THEORY\*

J. Engels<sup>1</sup>, F. Karsch<sup>1</sup>, and K. Redlich<sup>1,2</sup>

## ABSTRACT

The lattice data for the energy density of  $SU(2)$  gauge theory are calculated with non-perturbative derivatives of the coupling constants. These derivatives are obtained from two sources : i) a parametrization of the non-perturbative beta function in accord with the measured critical temperature and  $\Delta\beta$ -values and ii) a non-perturbative calculation of the pressure. We then perform a detailed finite size scaling analysis of the energy density near  $T_c$ . It is shown that at the critical temperature the energy density is scaling as a function of  $VT^3$  with the corresponding  $3d$  Ising model critical exponents. The value of  $\epsilon(T_c)/T_c^4$  in the continuum limit is estimated to be 0.256(23). In the high temperature regime the energy density is approaching its weak coupling limit from below, at  $T/T_c \approx 2$  it has reached only about 70% of the limit.

---

1 Fakultät für Physik, Universität Bielefeld, D-33615 Bielefeld, Germany

2 Institute for Theoretical Physics, University of Wrocław, PL-50205 Wrocław, Poland

\*Work supported by the Deutsche Forschungsgemeinschaft under research grant Pe 340/3-2 and the Bundesministerium für Forschung und Technologie (BMFT)

## 1. Introduction

The energy density for finite temperature  $SU(N)$  gauge systems is essential for the understanding and the investigation of the deconfinement transition and the plasma phase at high temperatures. In particular, a reliable estimate of the energy density  $\epsilon$  at the critical temperature  $T_c$  is needed for the design of heavy ion collision experiments aiming at the production of the quark-gluon plasma. For theory e. g., the high temperature behaviour of  $\epsilon$  is of interest for the test of and the connection to finite temperature perturbation theory. The determination of the correct non-perturbative energy density is therefore an important goal of Monte Carlo simulations.

The lattice calculations of  $\epsilon$  performed so far, though they are showing the same general behaviour for  $\epsilon$  on different size lattices, are not yet scaling, i. e. they do not lead to a unique function  $\epsilon(T)$ .

One of the sources of this disagreement has been addressed in [1] and is due to the use of weak coupling approximations to the derivatives with respect to the lattice anisotropy  $\xi = a/a_\tau$  ( $a$  and  $a_\tau$  are the lattice spacings in space and time directions) of the space-like ( $g_\sigma$ ) and time-like ( $g_\tau$ ) coupling constants. The derivatives appear in the lattice expressions for the pressure  $P$  and the energy density

$$\frac{\epsilon + P}{T^4} = 8NN_\tau^4 g^{-2} \left[ 1 - \frac{g^2}{2} \left( \frac{\partial g_\sigma^{-2}}{\partial \xi} - \frac{\partial g_\tau^{-2}}{\partial \xi} \right) \right] (P_\sigma - P_\tau) ; \quad (1)$$

$$\Delta \equiv \frac{\epsilon - 3P}{T^4} = 12NN_\tau^4 \left( \frac{\partial g_\sigma^{-2}}{\partial \xi} + \frac{\partial g_\tau^{-2}}{\partial \xi} \right) \left[ 2P_0 - (P_\sigma + P_\tau) \right] . \quad (2)$$

Here  $P_{\sigma,\tau}$  are the space and time plaquettes,  $P_{\sigma,\tau} = \frac{1}{N} \langle \text{Tr}(1 - U_1 U_2 U_3^\dagger U_4^\dagger) \rangle$ , on lattices of size  $N_\sigma^3 \times N_\tau$ . The plaquette  $P_0$  is measured on an  $N_\sigma^4$ -lattice and serves to normalize the interaction measure  $\Delta$  at  $T = 0$ . The derivatives have to be taken at  $\xi = 1$ . Their sum is related to the  $\beta$ -function through

$$\beta_f = -a \frac{dg}{da} = -g^3 \left( \frac{\partial g_\sigma^{-2}}{\partial \xi} + \frac{\partial g_\tau^{-2}}{\partial \xi} \right)_{\xi=1} . \quad (3)$$

Once the  $\beta$ -function and the pressure are known non-perturbatively, the energy density can be calculated with the appropriate non-perturbative derivatives.

This has been done in [1] for  $SU(3)$  and  $N_\sigma^3 \times 4$  lattices. In  $SU(2)$ , where much more data on lattices with various  $N_\sigma$  and  $N_\tau$  exist, this correction is still lacking. In the next two sections we shall therefore derive first a non-perturbative  $\beta$ -function for  $SU(2)$  and then the non-perturbative derivatives separately.

The other major effect on the energy density is coming from the finite size dependence on the spatial ( $N_\sigma$ ) and temporal ( $N_\tau$ ) extents of the lattice. Here we have to distinguish two regions of temperature or coupling constants. In the neighbourhood of the deconfinement transition we expect finite size scaling governed by the critical exponents of the transition and the increase of the correlation length. In the weak coupling or high temperature regime we expect a different behaviour of the energy density, which is dominated by the weak coupling expansion of  $\epsilon$  and its  $N_\sigma$ - and (stronger)  $N_\tau$ -dependence. We discuss the corresponding finite size equations in section 4.

We shall compare the available  $SU(2)$  data for the energy density after correction with non-perturbative coupling derivatives to the expectations from finite size scaling theory as described above. The results are presented and discussed in section 5.

## 2. Beta function and scaling in $SU(2)$ lattice gauge theory

It is well known, that physical quantities such as the critical temperature or the string tension are violating asymptotic scaling in the range of coupling constants considered so far in lattice calculations. Nevertheless the scaling of dimensionless ratios of observables works remarkably well [2] suggesting that deviations from asymptotic scaling may be described by a common non-perturbative  $\beta$ -function. To parametrize the corresponding non-perturbative dependence of the lattice spacing  $a$  on  $g^2$  we make the following ansatz

$$a\Lambda_L = R(g^2) \cdot \lambda(g^2) , \quad (4)$$

where

$$R(g^2) = \exp\left[-\frac{b_1}{2b_0^2} \ln(b_0 g^2) - \frac{1}{2b_0 g^2}\right] \quad (5)$$

is resulting from the integration of the two-loop weak coupling expansion of the  $\beta$ -function

$$-\beta_f = b_0 g^3 + b_1 g^5 + \dots \quad (6)$$

Here

$$b_0 = \frac{11N}{48\pi^2} \quad , \quad b_1 = \frac{34}{3} \left( \frac{N}{16\pi^2} \right)^2 \quad (7)$$

are scheme independent. The inclusion of terms of order  $O(g^7)$  in the expansion of the  $\beta$ -function is then equivalent to a deviation of  $\lambda$  from unity.

The relation of the correction factor  $\lambda$  to the sum of non-perturbative derivatives is found by rewriting Eq. (3) as

$$\frac{dg^{-2}}{d \ln a} = -2 \left( \frac{\partial g_\sigma^{-2}}{\partial \xi} + \frac{\partial g_\tau^{-2}}{\partial \xi} \right)_{\xi=1} \quad , \quad (8)$$

and using

$$\frac{d \ln a}{dg^{-2}} = -\frac{1}{2b_0} + \frac{b_1}{2b_0^2} g^2 + \frac{d \ln \lambda}{dg^{-2}} \quad . \quad (9)$$

It is then convenient to write  $\lambda$  for small  $g^2$  in the following asymptotic form

$$\lambda(g^2) = \exp \left[ \frac{1}{2b_0^2} (c_1 g^2 + c_2 g^4 + c_3 g^6 + \dots) \right] \quad , \quad (10)$$

which implies  $\lambda(0) = 1$ .

The function  $\lambda$  may be determined from any measured quantity of non-zero dimension. However only for small enough values of  $g^2$  one may hope to find a unique function from different observables.

In  $SU(2)$  lattice gauge theory we shall exploit the measurements of the critical coupling constant  $g_c^2$  for  $N_\tau = 2, 3, 4, 5, 6, 8, 16$  [2,3,4] to derive  $\lambda$ . From the  $g_c^2$ -values we find the critical temperature  $T_c$ . On a lattice with  $N_\tau$  points in the temporal direction the temperature is

$$T = \frac{1}{N_\tau a} \quad . \quad (11)$$

Therefore we have

$$\lambda(g_c^2) = \frac{1}{N_\tau R(g_c^2) \cdot T_c / \Lambda_L} \quad . \quad (10)$$

Demanding independence of  $g^2$  for  $T_c/\Lambda_L$  allows us then to determine the function  $\lambda(g^2)$  in the presently studied coupling regime. In Fig. 1 we show the critical temperature  $1/(N_\tau R)$  as calculated from the two-loop formula, Eq. (5), i. e. by assuming  $\lambda = 1$ , at the measured critical coupling for various  $N_\tau$ .

It has been noted [2,5,6] that the deviations from asymptotic scaling, which are obvious from Fig. 1 can, to a large extent, be accounted for by the introduction of an effective coupling constant.

For our present analysis of bulk thermodynamics it is, however, more convenient to achieve a parametrization of the scaling violations in terms of the bare coupling constant. This has the advantage of giving us directly the  $\beta$ -function, which we need anyhow for the evaluation of the energy density and the pressure.

We thus proceed in the following way. First we use only those points, which belong to the weak coupling regime ( $4/g^2 > 2.23$ , i. e.  $N_\tau \geq 4$ ) to make a fit to  $1/(N_\tau R)$  with the asymptotic form, Eq. (10), of  $\lambda$ . We have tried various possibilities for the exponent of  $\lambda$  in Eq. (10). A rather good fit is obtained with the simple parametrization

$$c_1 \equiv c_2 \equiv c_{n>3} \equiv 0 , \quad (12)$$

so that

$$\lambda_{as} = \exp \left[ \frac{c_3 g^6}{2b_0^2} \right] . \quad (13)$$

The best result is given by  $c_3 = 5.529(63) \cdot 10^{-4}$ , which leads to

$$T_c/\Lambda_L = 21.45(14) . \quad (14)$$

The last number is compatible with a corresponding extrapolation to  $a = 0$  in ref.[2].

The simple asymptotic fit Eq. (13) deviates in the neighbourhood of the crossover point from the measured two-loop critical temperature values, as can be seen in Fig. 1. In a second step we have therefore essentially fitted the measured points with a Spline interpolation, which continuously extends into the region, where Eq. (13) is valid. The solid line in Fig. 1 shows the final interpolation and the ratio of the measured  $1/(N_\tau R(g_c^2))$  over the fitted  $\lambda(g_c^2)$ . The ratio should be a constant and equal to  $T_c/\Lambda_L$ . In Table 1 we give  $\lambda$  and the derivative from Eq. (8), which up to a factor (-2) equals to the sum of derivatives. The latter is shown in Fig. 2.

$4/g^2$	$\lambda$	$adg^{-2}/da$	$dg_{\sigma}^{-2}/d\xi$	$dg_{\tau}^{-2}/d\xi$
2.15	1.913188	-.137878	.571969	-.503031
2.20	1.964628	-.117386	.377374	-.318682
2.25	1.983554	-.099932	.283626	-.233660
2.26	1.982803	-.096746	.265652	-.217279
2.27	1.980406	-.093647	.246364	-.199541
2.28	1.976305	-.090631	.223386	-.178070
2.29	1.970443	-.087694	.210139	-.166292
2.30	1.962762	-.084833	.204750	-.162334
2.31	1.953283	-.082321	.201087	-.159927
2.32	1.942236	-.080266	.198051	-.157918
2.33	1.929886	-.078616	.195733	-.156425
2.34	1.916495	-.077331	.193934	-.155269
2.35	1.902327	-.076385	.192421	-.154228
2.36	1.887647	-.075764	.191102	-.153220
2.37	1.872718	-.075460	.189937	-.152207
2.38	1.857789	-.075402	.188928	-.151227
2.39	1.842973	-.075403	.188076	-.150375
2.40	1.828310	-.075456	.187333	-.149604
2.41	1.813840	-.075563	.186643	-.148862
2.42	1.799604	-.075726	.185993	-.148130
2.43	1.785641	-.075944	.185374	-.147402
2.44	1.771977	-.076183	.184775	-.146683
2.45	1.758616	-.076435	.184202	-.145985
2.50	1.696441	-.077883	.182826	-.143884
2.55	1.642101	-.079563	.182356	-.142575
2.60	1.595003	-.081199	.182339	-.141739
2.65	1.554151	-.082690	.182157	-.140811
2.70	1.518180	-.083756	.181851	-.139974
2.75	1.485366	-.084280	.181587	-.139447
2.80	1.454568	-.084734	.181364	-.138997
$\infty$	1.000000	-.092878	.114025	-.067586

**Table 1**

The correction factor  $\lambda$  and non-perturbative coupling derivatives.

The interpolation was checked further by a comparison of the coupling constant shift  $\Delta\beta$  to MCRG measurements with scale two blocking transformations [7,8]. In Fig. 3 the data and our  $\Delta\beta$  are shown together with the two-loop prediction. At high  $\beta$ -values the measurements from the small ( $8^4$ ) lattice blocking are slightly

inconsistent with those on a large ( $32^4$ ) lattice. Our result prefers the large lattice data and is, in contrast to the two-loop function, in full agreement with the rest of the data. In addition we have included in the figure data derived from the critical couplings  $g_c^2$  of the deconfinement transition for  $N_\tau$ -values, which differ by a factor two. They are of course coinciding with our curve.

### 3. The non-perturbative coupling derivatives

The non-perturbative  $\beta$ -function, which we have just derived, yields one of the two equations for the determination of the non-perturbative coupling derivatives. Another one is found by expressing, via Eqs. (1) and (2), the pressure in terms of the derivatives

$$\frac{P}{T^4} = NN_\tau^4 \left\{ \left[ 2g^{-2} - \left( \frac{\partial g_\sigma^{-2}}{\partial \xi} - \frac{\partial g_\tau^{-2}}{\partial \xi} \right) \right] (P_\sigma - P_\tau) - 3 \left( \frac{\partial g_\sigma^{-2}}{\partial \xi} + \frac{\partial g_\tau^{-2}}{\partial \xi} \right) \left[ 2P_0 - (P_\sigma + P_\tau) \right] \right\}. \quad (15)$$

In ref.[1] it was demonstrated how the pressure may be calculated as well non-perturbatively without derivatives, at least on large lattices. To this end one has to calculate the normalized free energy density from

$$\frac{f}{T^4} \Big|_{\beta_0}^\beta = -3N_\tau^4 \int_{\beta_0}^\beta d\beta' \left[ 2P_0 - (P_\sigma + P_\tau) \right], \quad (16)$$

where  $\beta = 4/g^2$ , and to use the identity

$$P = -f, \quad (17)$$

which is valid for homogeneous systems. It was checked for  $SU(2)$  [1] that a lattice of size  $18^3 \times 4$  ( where we have many data points ) is large enough to justify this approximation. We have taken advantage of this fact and first calculated the pressure non-perturbatively on the  $18^3 \times 4$  lattice by interpolating and integrating over  $[2P_0 - (P_\sigma + P_\tau)]$ . Subsequently we used Eqs. (8) and (15) to obtain

$$\frac{\partial g_\sigma^{-2}}{\partial \xi} = g^{-2} - \frac{1}{4} \frac{dg^{-2}}{d \ln a} + \frac{1}{(P_\sigma - P_\tau)} \left( -\frac{P}{2NN_\tau^4 T^4} + \frac{3}{4} \frac{dg^{-2}}{d \ln a} [2P_0 - (P_\sigma + P_\tau)] \right), \quad (18)$$

and

$$\frac{\partial g_\tau^{-2}}{\partial \xi} = -\frac{\partial g_\sigma^{-2}}{\partial \xi} - \frac{1}{2} \frac{dg^{-2}}{d \ln a}, \quad (19)$$

separately. It is clear, that below the critical point ( $4/g^2 < 2.30$ ), where both the pressure  $P$  and the plaquette difference  $P_\sigma - P_\tau$  are small, the error on  $\partial g_\sigma^{-2}/\partial\xi$  becomes relatively large. We have therefore smoothly interpolated the values in that region. The resulting non-perturbative derivatives have been listed in Table 1. We observe strong deviations from the asymptotic predictions [9] up to large values of the coupling ( $4/g^2 \simeq 3.0$ ).

#### 4. Finite size scaling behaviour

##### A. The phase transition region

On a finite lattice the correlation length is limited by the characteristic length scale of the system, i. e. normally the spatial extension  $N_\sigma$ . This limitation prevents the divergence of the correlation length at the critical point of a second order deconfinement transition. As a consequence the thermodynamic observables exhibit close to the transition finite size scaling properties, which are determined by the critical exponents and the length scale. According to the universality hypothesis of Svetitsky and Yaffe [10] the exponents of  $SU(2)$  should be the same as those of the three-dimensional Ising model.

Usually finite size scaling analyses are carried out at fixed  $N_\tau$ , but varying  $N_\sigma$ , see e. g. ref.[3]. The spatial extension determines then obviously the scale. In investigations, where results from lattices with varying  $N_\sigma$  and  $N_\tau$  are compared, the dimensionless ratio

$$\frac{N_\sigma}{N_\tau} = LT, \quad (20)$$

where  $L = N_\sigma a$ , has turned out to be the appropriate variable. This was observed already in studies of the heavy quark potential [11], and later on confirmed by the behaviour of the Binder cumulant [2].

We may check this idea further by looking at the interaction measure  $\Delta$ , Eq. (2), for various  $N_\sigma$  and  $N_\tau$  in the neighbourhood of the critical point, as a function of  $T/T_c$ . Note, that here the non-perturbative  $\beta$ -function enters in both the quantity  $\Delta$  and the scale  $T/T_c$ , but no single coupling derivative. In Fig. 4 we see a clear coincidence of  $\Delta$ -data belonging to the same ratio  $N_\sigma/N_\tau$ .

The finite size dependence of the energy density is related to the singular part  $f_s$  of the free energy density. Since the critical exponent  $\alpha$  of the specific heat is relatively small ( $\alpha \approx 0.11$ ) [3], one expects that the regular parts in the specific



heat and in the energy density are dominating. Correspondingly, we make the following ansatz for the energy density close to  $T_c$

$$\frac{\epsilon}{T^4} = \left(\frac{\epsilon}{T^4}\right)_{reg} + \left(\frac{N_\sigma}{N_\tau}\right)^{(\alpha-1)/\nu} Q_\epsilon \left(t \left(\frac{N_\sigma}{N_\tau}\right)^{1/\nu}\right), \quad (21)$$

where we have already neglected irrelevant scaling fields. Here

$$t = (T - T_c)/T_c \quad (22)$$

is the reduced temperature,  $Q_\epsilon$  the scaling function of the energy density and  $\nu$  the critical exponent of the correlation length.

### B. The weak coupling region

For small bare couplings  $g^2$ , in the vicinity of the continuum limit, the energy density may be approximated by its weak coupling expansion. To obtain it up to order  $g^2$ , we first derive  $\epsilon/T^4$  from Eqs. (1) and (2)

$$\begin{aligned} \frac{\epsilon}{T^4} = 3NN_\tau^4 \left\{ \left[ 2g^{-2} - \left( \frac{\partial g_\sigma^{-2}}{\partial \xi} - \frac{\partial g_\tau^{-2}}{\partial \xi} \right) \right] (P_\sigma - P_\tau) \right. \\ \left. + \left( \frac{\partial g_\sigma^{-2}}{\partial \xi} + \frac{\partial g_\tau^{-2}}{\partial \xi} \right) \left[ 2P_0 - (P_\sigma + P_\tau) \right] \right\}. \end{aligned} \quad (23)$$

Into this equation we insert the weak coupling expansions of the plaquettes for  $SU(N)$  lattice gauge theory [12]

$$P = g^2 \frac{N^2 - 1}{N} P^{(2)} + g^4 (N^2 - 1) P^{(4a)} + g^4 \frac{(2N^2 - 3)(N^2 - 1)}{N^2} P^{(4b)} + O(g^6), \quad (24)$$

and the asymptotic values of the coupling derivatives [9]

$$\begin{aligned} \frac{\partial g_\sigma^{-2}}{\partial \xi} - \frac{\partial g_\tau^{-2}}{\partial \xi} &= \frac{N^2 - 1}{N} \cdot 0.146711 - N \cdot 0.019228, \\ \frac{\partial g_\sigma^{-2}}{\partial \xi} + \frac{\partial g_\tau^{-2}}{\partial \xi} &= b_0 = \frac{11N}{48\pi^2}. \end{aligned} \quad (25)$$

The coefficients of the perturbative formula

$$\frac{\epsilon}{T^4} = a_0 + a_1 g^2 + O(g^4), \quad (26)$$

are related to those of the plaquettes in the following way

$$\begin{aligned}
a_0 &= 6(N^2 - 1)N_\tau^4 \Delta P_{\sigma\tau}^{(2)} , \\
a_1 &= 6(N^2 - 1)N_\tau^4 \left\{ N \Delta P_{\sigma\tau}^{(4a)} + \frac{2N^2 - 3}{N} \Delta P_{\sigma\tau}^{(4b)} - 0.146711 \frac{N^2 - 1}{2N} \Delta P_{\sigma\tau}^{(2)} \right. \\
&\quad \left. + 4N [ 0.000499 \Delta P_{0\sigma}^{(2)} + 0.005306 \Delta P_{0\tau}^{(2)} ] \right\} , \tag{27}
\end{aligned}$$

where

$$\Delta P_{\alpha\beta} = P_\alpha - P_\beta , \tag{28}$$

was used as an abbreviation and  $P_0$  is the plaquette on the respective symmetric  $N_\sigma^4$  lattice. The coefficients  $a_0, a_1$  approach with increasing  $N_\sigma$  and  $N_\tau$  the corresponding continuum values

$$\begin{aligned}
a_0 &= \frac{\pi^2}{15} (N^2 - 1) , \\
a_1 &= -\frac{1}{48} (N^2 - 1) N . \tag{29}
\end{aligned}$$

We have calculated both coefficients on a large number of  $N_\sigma^3 \times N_\tau$  lattices. In Figs. 5 and 6 they are plotted for  $SU(2)$  at fixed ratios  $N_\sigma/N_\tau$  as a function of  $N_\tau$ . We observe, that  $a_0$  has essentially the same  $N_\tau$ -dependence for all ratios  $N_\sigma/N_\tau$  and that the thermodynamic limit  $N_\sigma \rightarrow \infty$  is almost reached already for  $N_\sigma/N_\tau > 4$ . For a lattice calculation with an energy density as close as possible to the continuum limit one should therefore choose  $N_\tau$  as large as possible at a moderate ratio  $N_\sigma/N_\tau$ .

Asymptotically, for  $N_\sigma \rightarrow \infty$  and large  $N_\tau$  the leading terms of  $a_0$  are given for  $SU(N)$  by

$$a_0 = (N^2 - 1) \left[ \frac{\pi^2}{15} + \frac{2\pi^4}{63} \cdot \frac{1}{N_\tau^2} + O\left(\frac{1}{N_\tau^4}\right) \right] . \tag{30}$$

The  $N_\sigma$ - and  $N_\tau$ -dependences of  $a_1$  are more complicated. For  $N_\sigma \rightarrow \infty$  and large  $N_\tau$  the second coefficient approaches the continuum value from below, in contrast to  $a_0$ . For fixed  $N_\sigma/N_\tau$ , both  $a_0$  and  $a_1$  cross their respective continuum limit lines, but at different  $N_\tau$ -values.

## 5. Numerical results for the energy density

With our results for the non-perturbative derivatives and the  $\beta$ -function we are now able to reevaluate the energy density with the plaquette values from refs. [3,4]. In Fig. 7 we show  $\epsilon/T^4$  in the vicinity of the deconfinement transition as a function of  $T/T_c$ . Like in the case of the interaction measure  $\Delta$  we observe that at fixed temperature  $\epsilon/T^4$  depends only on the ratio  $N_\sigma/N_\tau$ . From the ansatz, Eq. (21), the following scaling behaviour is then expected at  $t = 0$

$$\frac{\epsilon}{T^4} = \left( \frac{\epsilon}{T^4} \right)_\infty + \left( \frac{N_\sigma}{N_\tau} \right)^{(\alpha-1)/\nu} \cdot Q_\epsilon(0) . \quad (31)$$

We have made fits of this form to data at  $T_c$  coming from seven different lattice sizes. Fixing the critical exponents to those of the 3d Ising model, i. e.

$$(\alpha - 1)/\nu = -1.41 , \quad (32)$$

we find for the value of the energy density in the limit  $N_\sigma/N_\tau \rightarrow \infty$  ( the regular term at  $T_c$  )

$$\left( \frac{\epsilon}{T^4} \right)_\infty = 0.256(23) . \quad (33)$$

Our result is somewhat lower than the one found previously in ref. [13], where perturbative derivatives were used. A plot of the fit and the data are shown in Fig. 8. If we consider the exponent of  $(N_\sigma/N_\tau)$  in Eq. (31) as a free parameter we find as best value

$$(\alpha - 1)/\nu = -1.58 . \quad (34)$$

This entails a slight change in the continuum limit value, Eq. (33), which however was already taken into account in the error estimate.

In the confined, low temperature phase an often used model for the energy density is that of a free gas of massive glueballs of various spins and parities. Assuming Boltzmann statistics the energy density of such a glueball gas is given by

$$\frac{\epsilon_{gb}(T)}{T^4} = \frac{1}{2\pi^2} \sum_i d_i \left( \frac{M_i}{T} \right)^3 \left[ K_1 \left( \frac{M_i}{T} \right) + \frac{3T}{M_i} K_2 \left( \frac{M_i}{T} \right) \right] . \quad (35)$$

In pure  $SU(2)$  lattice gauge theory the following glueball states have been identified :  $M_{O+}/T_c \sim 5.5$ ,  $M_{2+}/T_c \sim 8.0$ ,  $M_{O-}/T_c \sim 9.5$ , and  $M_{2-}/T_c \sim 10.2$  [14]. At the critical temperature the energy density of an ideal gas of these glueballs is then found to be

$$\epsilon_{gb}(T_c)/T_c^4 = 0.050 , \quad (36)$$

i. e. a factor five less than our estimate, Eq. (33). The presence of strong glueball interactions is therefore to be expected in the confinement phase.

Comparing the critical energy density with that of an asymptotically free gluon gas

$$\epsilon_g(T)/T^4 = \pi^2/5 , \quad (37)$$

we find a difference of nearly a factor eight. This means, that also in the deconfinement phase close to the transition strong interactions of the constituents of the gluon plasma are anticipated.

$4/g^2$	$N_{meas}$	$P_\sigma$	$P_\tau$	$\langle  L  \rangle$
2.55	24840	.3384811(34)	.3384526(34)	.07344(19)
2.60	17750	.3298618(39)	.3298233(37)	.09524(11)
2.65	42304	.3218638(23)	.3218192(22)	.11147(06)
2.74	91900	.3086725(15)	.3086204(14)	.13600(04)

**Table 2**

Results from Monte Carlo calculations on a  $32^3 \times 8$  lattice.

Let us now consider the high temperature phase. In Fig. 9a we show the approach of the energy density to the leading weak coupling term  $a_0 = \epsilon^{wc}/T^4$  - the lattice Stefan-Boltzmann limit - for two lattices. The  $32^3 \times 8$  data are new. Here the lattice size was chosen such as to have a large  $N_\tau$ -value and a reasonable  $N_\sigma/N_\tau$ -ratio at the same time. Details of these data are presented in Table 2. We see from Fig. 9a that the data even at  $T/T_c \approx 2$  are still about 30% below that of a gas of non-interacting  $SU(2)$  gluons and that the deviations from it at fixed temperature are only slightly  $N_\tau$ -dependent. Yet, we are still not in the weak coupling region, since the differences cannot be explained by the next-to-leading order weak coupling term. This does not come as a surprise, because in the  $T$ -range shown, the coupling derivatives are still non-perturbative.

In Fig. 9b we have plotted the difference between  $\epsilon^{wc}/T^4$  and the energy density data, showing again that the lattice Stefan-Boltzmann limit is clearly approached from below. A comparison of  $(\epsilon^{wc} - \epsilon)/T^4$  to finite temperature perturbation theory with only one term proportional to the temperature dependent running coupling constant leads to a large value for  $g^2(T)$  of the order of  $4 \sim 5$ . It seems therefore that at presently accessible temperature values low order perturbation theory is not applicable.

## 6. Conclusions and discussion

We have studied the finite size scaling behaviour of the energy density in  $SU(2)$  gauge theory at finite temperature. We find that the energy density at the critical point is only about 1/8 of the ideal gas value and also at  $T \simeq 2T_c$  it is still 30% below this limit. The discrepancy between this result and earlier findings of a rapid approach to the ideal gas limit can be traced back to our non-perturbative definition of the pressure, Eq. (16). The additional use of a non-perturbative  $\beta$ -function in the definition of  $(\epsilon - 3P)/T^4$  is a minor modification to this. In fact the non-perturbative calculation of  $P/T^4$  through Eq. (16) yields above  $T_c$  a smaller value than Eq. (15) with perturbative coupling derivatives. This is reflected in a strong deviation of our results for  $\partial g_{\sigma, \tau}^{-2}/\partial \xi$  from the perturbative values ( see Table 1). A similar result was obtained in  $SU(3)$ , where these derivatives were directly calculated from Wilson loops on anisotropic lattices [15].

Some uncertainty on the absolute value of the pressure and consequently also the energy density is due to our approximation  $P/T^4 \equiv 0$  for  $T \simeq 0.8T_c$ . This is suggested by the Monte Carlo data and seems also justified because the confinement phase consists only of heavy glueball states. We also note that unlike in the perturbative definition of thermodynamic quantities the non-perturbative approach does not automatically ensure that the ideal gas limit is reached for  $4/g^2 \rightarrow \infty$ . However, it was checked in [1], that the order  $g^2$  correction to Eq. (16) in the infinite temperature limit has the correct perturbative form.

In the near future more Monte Carlo calculations in the high temperature region are needed to clarify the nature of the approach to the region where finite temperature perturbation theory is valid.

**Acknowledgements:** We are indebted to the HLRZ Jülich for providing the necessary computer time. We thank J. Rank for the data from his simulations on the  $32^3 \times 8$  lattice. K. R. acknowledges support by the Stabsabteilung Internationale Beziehungen, KFA Karlsruhe and Komitet Badań Navkowych (KBN). One of us (K. R.) is indebted to H. Satz for interesting discussions and suggestions.

### References

- 1) J. Engels, J. Fingberg, F. Karsch, D. Miller and M. Weber, Phys. Lett. B252 (1990) 625.
- 2) J. Fingberg, U. Heller and F. Karsch, Nucl. Phys. B392 (1993) 493.
- 3) J. Engels, J. Fingberg and M. Weber, Nucl. Phys. B332 (1990) 737.
- 4) J. Engels, J. Fingberg and D. E. Miller, Nucl. Phys. B387 (1992) 501.
- 5) K. Akemi et al. Phys. Rev. Lett. 71 (1993) 3063.
- 6) A. X. El-Khadra, G. Hockney, A. S. Kronfeld and P. B. Mackenzie, Phys. Rev. Lett. 69, (1992) 729;
- 7) U. Heller and F. Karsch, Phys. Rev. Lett. 54 (1985) 1765.
- 8) K. M. Decker and P. de Forcrand, Nucl. Phys. B(Proc. Suppl.) 17 (1990) 567.
- 9) F. Karsch, Nucl. Phys. B205 (1982) 285.
- 10) B. Svetitsky and G. Yaffe, Nucl. Phys. B210 [FS6] (1982) 423.
- 11) J. Engels, F. Karsch and H. Satz, Nucl. Phys. B315 (1989) 419.
- 12) U. Heller and F. Karsch, Nucl. Phys. B251 [FS13] (1985) 254.
- 13) J. Engels, J. Fingberg and V. Mitrjushkin, Phys. Lett. B298 (1993) 154.
- 14) C. Michael and M. Teper, Phys. Lett. B199 (1987) 95.
- 15) G. Burgers, F. Karsch, A. Nakamura and I. O. Stamatescu, Nucl. Phys. B304 (1988) 587.

**Figure Captions:**

1. The measured critical temperature  $1/(N_\tau R)$  for  $\lambda = 1$  (circles) and  $T_c/\Lambda_L$  (squares) obtained after correction with the factor  $\lambda$ , vs.  $4/g^2$  for different  $N_\tau$ . The solid line results from our interpolation of  $\lambda$ , the dashed-dotted line from the asymptotic form  $\lambda_{as}$ . The dashed line is the fit result from Eq. (14).
2. The sum of derivatives  $(\partial g_\sigma^{-2}/\partial\xi + \partial g_\tau^{-2}/\partial\xi)$  at  $\xi = 1$ . The solid line is our non-perturbative result, the dashed-dotted line comes from  $\lambda_{as}$  and the dashed line from the two-loop approximation.
3. The coupling constant shift  $\Delta\beta$  from scale two blocking transformations vs.  $4/g^2$ , plotted at the larger of the two values. The data were measured by using two different lattices (diamonds, triangle) [7], blocking on one large lattice (crosses) [8] or obtained from  $T_c$  (circles) [2]. The notation of the lines is the same as in Fig. 2.
4. The interaction measure  $\Delta = (\epsilon - 3P)/T^4$  for various  $N_\sigma$  and  $N_\tau$  in the neighbourhood of the critical point, as a function of  $T/T_c$ . The necessary plaquette data were taken from refs.[3,4].
5. The first coefficient  $a_0$  of the weak coupling expansion of  $\epsilon/T^4$  versus  $N_\tau^{-2}$  for the fixed ratios  $N_\sigma/N_\tau = 2, 4, 8, 16$  (long dashes, dotted-dashed, dotted and solid lines). The continuum value is shown as a line of short dashes; the leading term in  $N_\tau^{-2}$  as a solid straight line. All numbers are for  $SU(2)$ .
6. The second coefficient  $a_1$  of the weak coupling expansion of  $\epsilon/T^4$  versus  $N_\tau$  for the fixed ratios  $N_\sigma/N_\tau = 2, 4, 6, 8$  (long dashes, dotted-dashed, solid and dotted lines). The continuum value is shown as a line of short dashes. All numbers are for  $SU(2)$ .
7. The energy density  $\epsilon/T^4$  for various  $N_\sigma$  and  $N_\tau$  in the neighbourhood of the critical point, as a function of  $T/T_c$ .
8. The energy density at  $T_c$  as a function of  $(N_\sigma/N_\tau)^{(\alpha-1)/\nu}$  with the critical exponents from the 3d Ising model. The straight line is a fit with the scaling form, Eq. (31). The notation for the data is like in Fig. 7, the diamond is from a  $26^3 \times 4$  lattice.
9. Comparison of the leading term of the weak coupling expansion  $a_0 = \epsilon^{wc}/T^4$  to data for  $\epsilon/T^4$  on two different lattices, versus  $T/T_c$ . Fig. 9a shows the data directly, Fig. 9b the difference to the respective weak coupling limit.

This figure "fig1-1.png" is available in "png" format from:

<http://arxiv.org/ps/hep-lat/9408009v1>



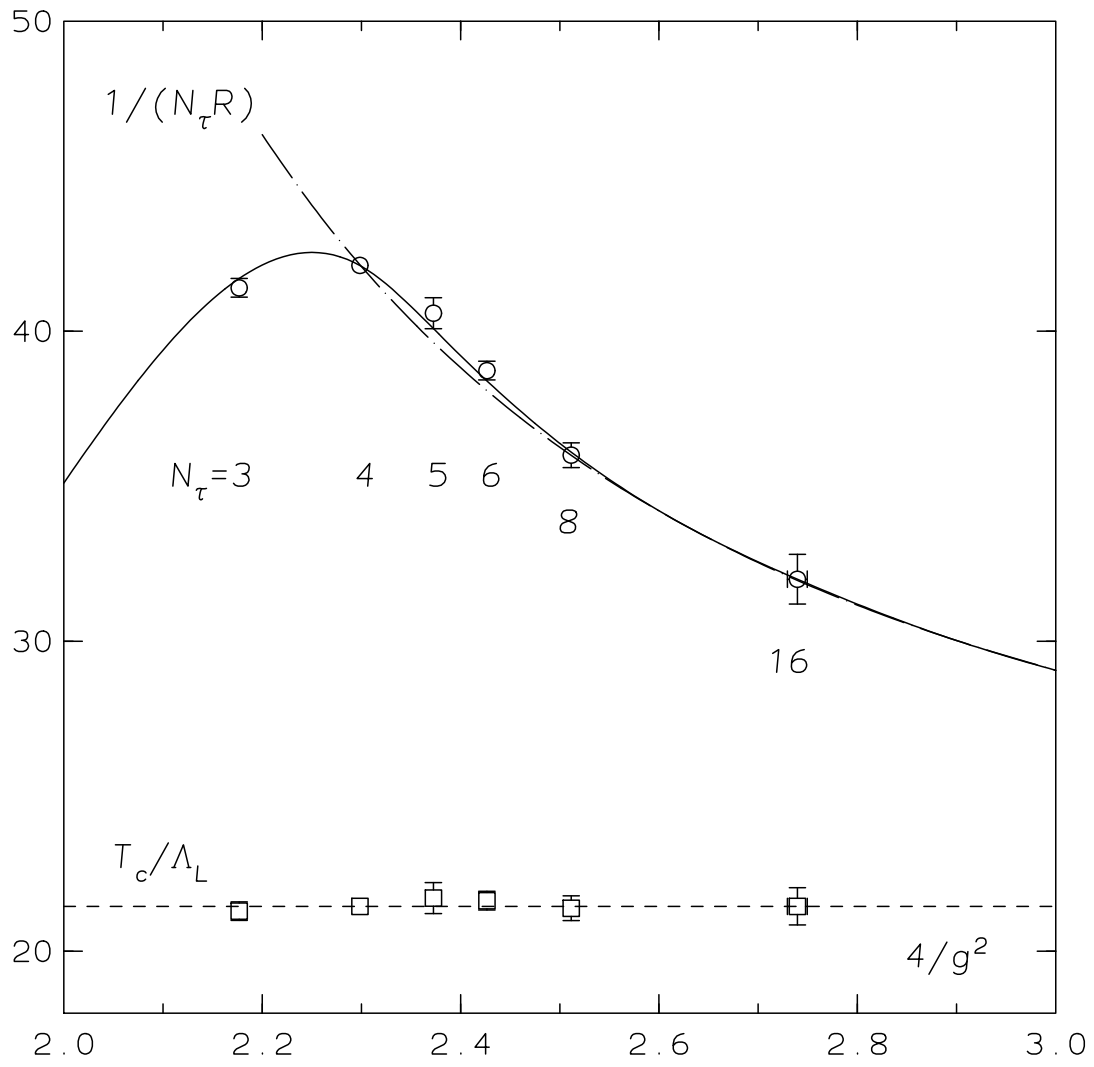


Figure 1

This figure "fig2-1.png" is available in "png" format from:

<http://arxiv.org/ps/hep-lat/9408009v1>

This figure "fig1-2.png" is available in "png" format from:

<http://arxiv.org/ps/hep-lat/9408009v1>

This figure "fig2-2.png" is available in "png" format from:

<http://arxiv.org/ps/hep-lat/9408009v1>

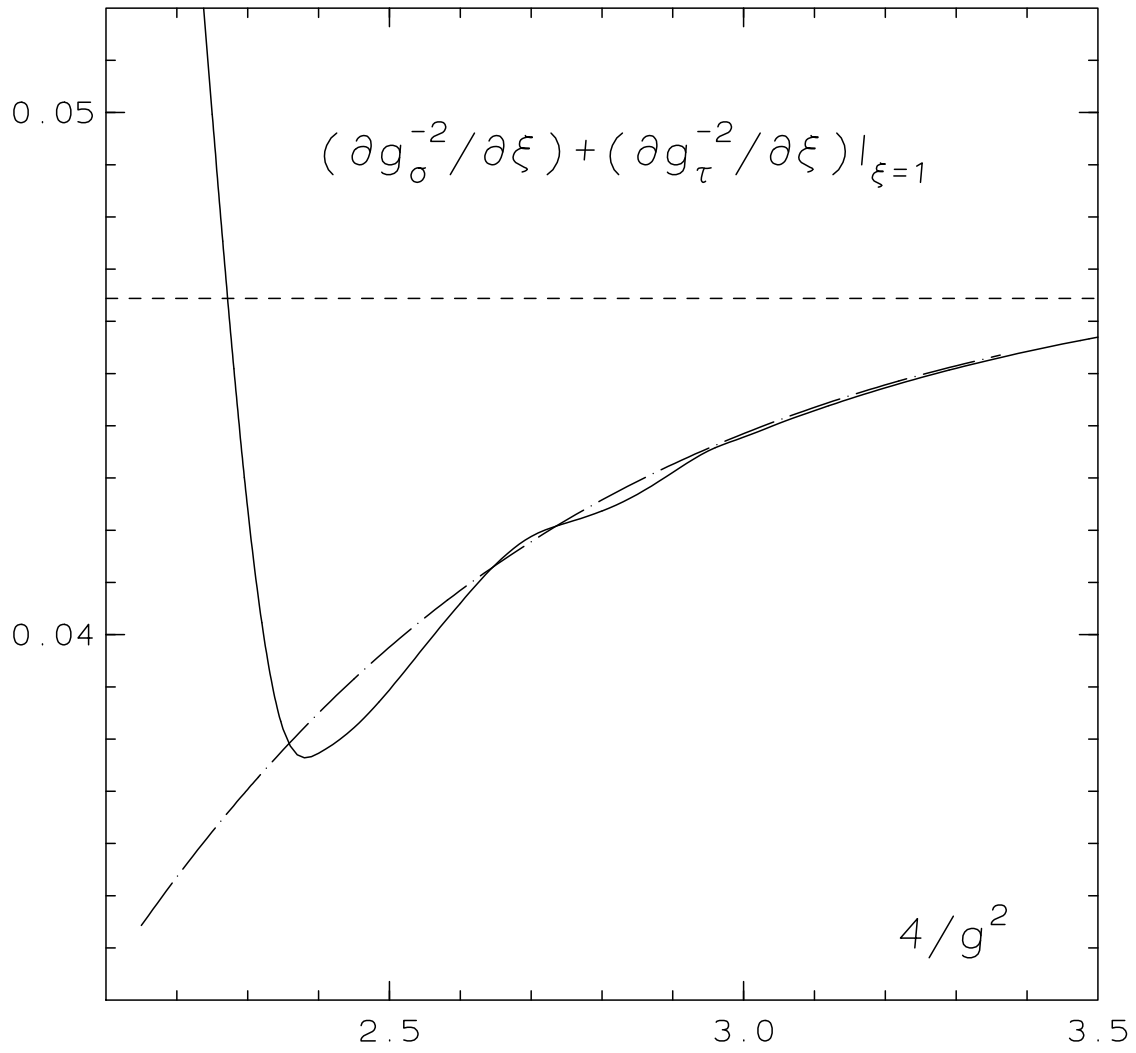


Figure 2

This figure "fig1-3.png" is available in "png" format from:

<http://arxiv.org/ps/hep-lat/9408009v1>

This figure "fig2-3.png" is available in "png" format from:

<http://arxiv.org/ps/hep-lat/9408009v1>

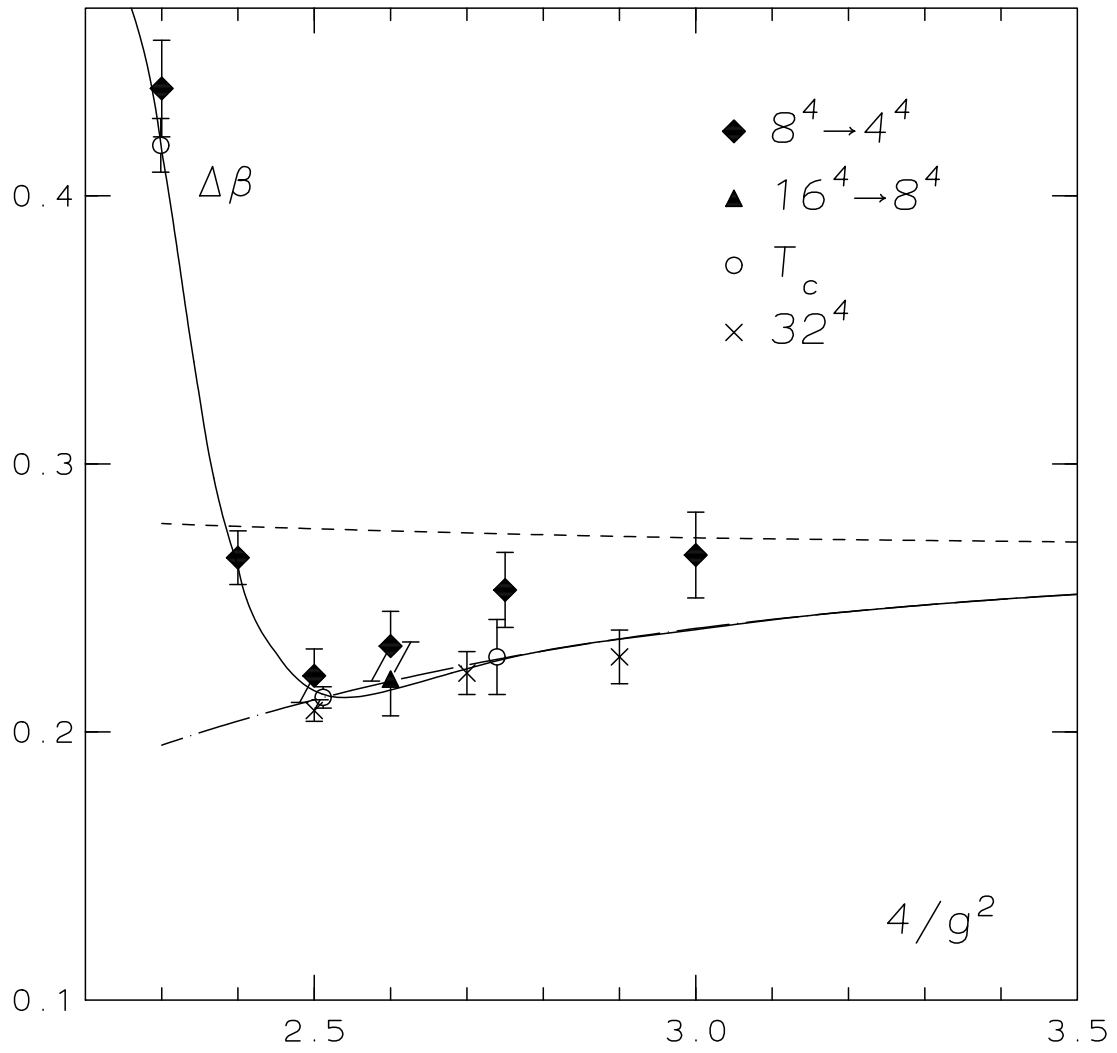


Figure 3



This figure "fig1-4.png" is available in "png" format from:

<http://arxiv.org/ps/hep-lat/9408009v1>

This figure "fig2-4.png" is available in "png" format from:

<http://arxiv.org/ps/hep-lat/9408009v1>

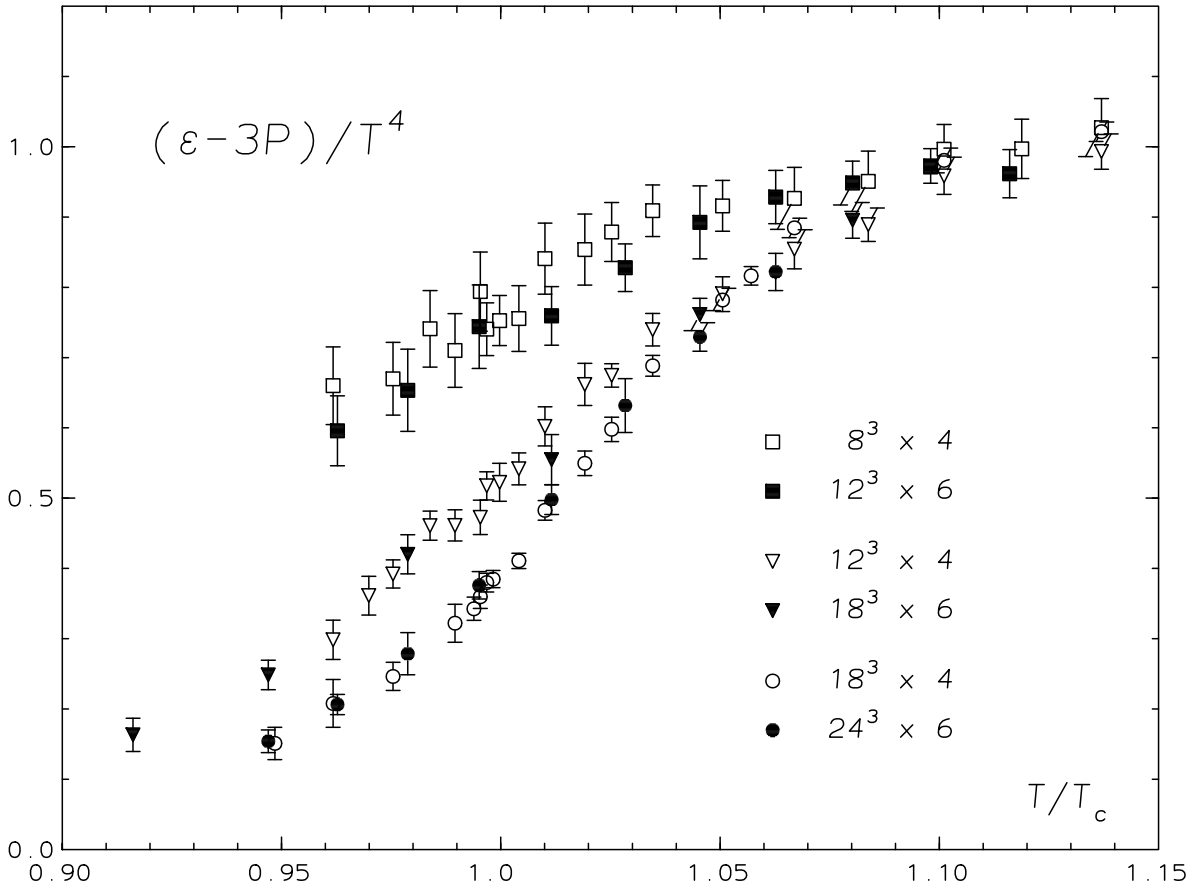


Figure 4

This figure "fig1-5.png" is available in "png" format from:

<http://arxiv.org/ps/hep-lat/9408009v1>

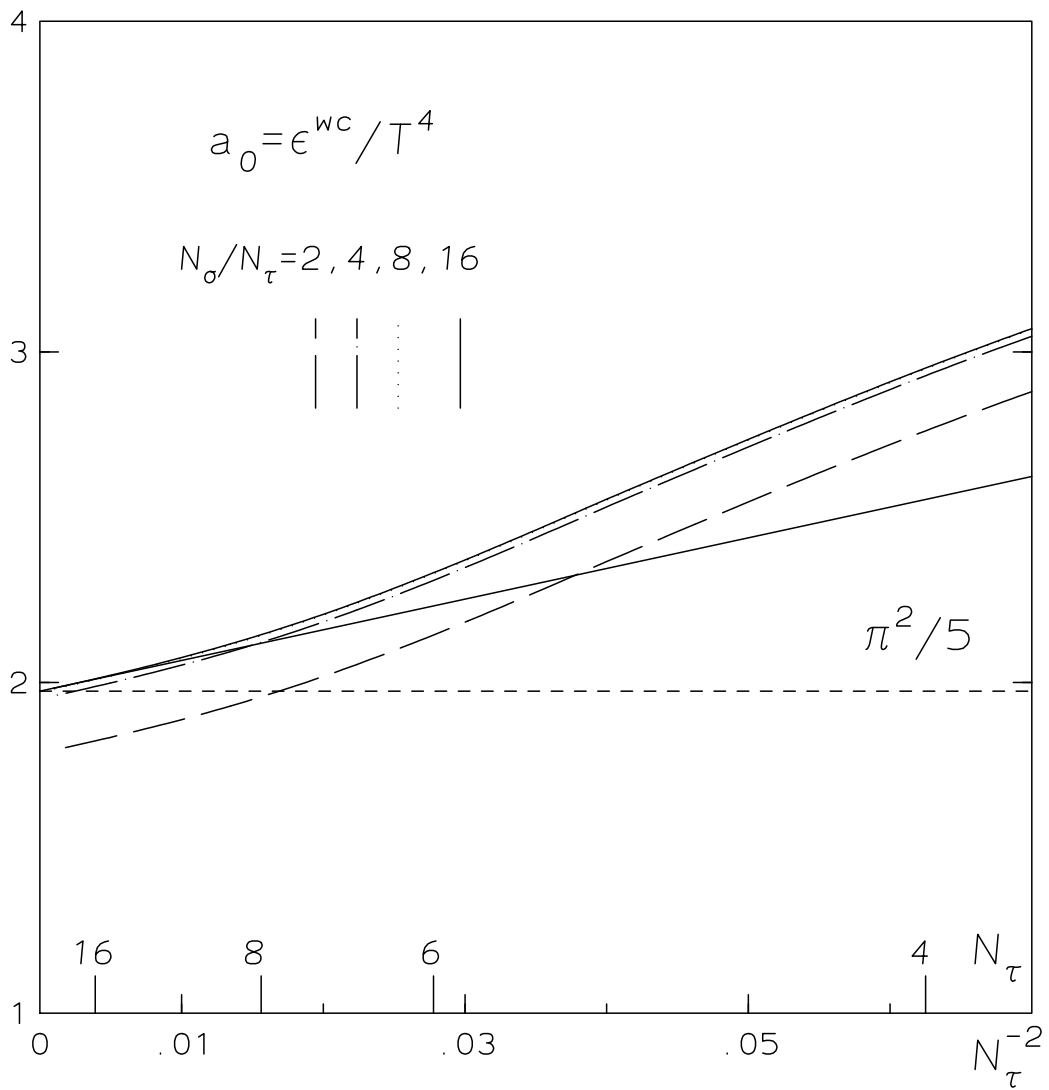


Figure 5

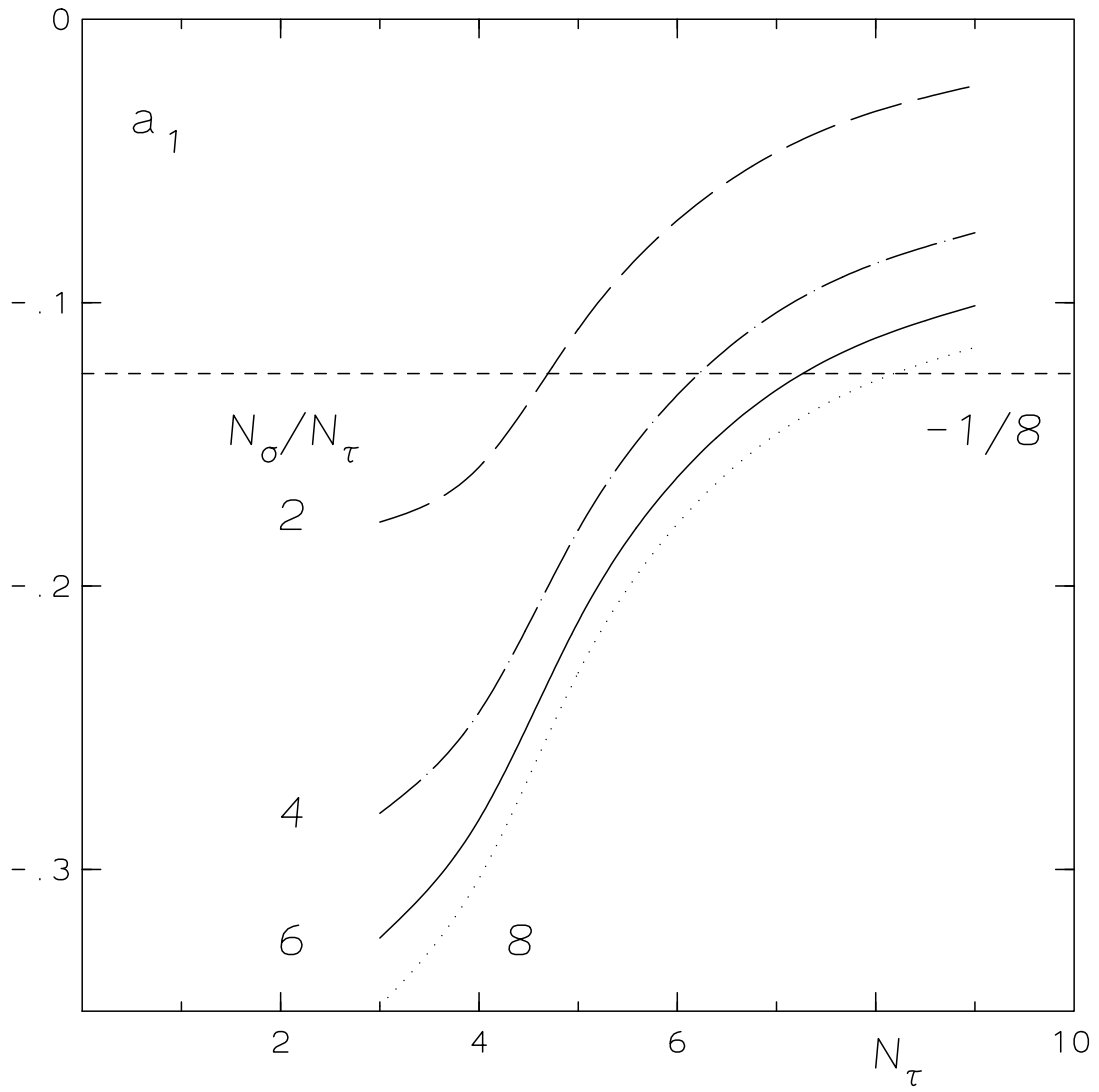


Figure 6

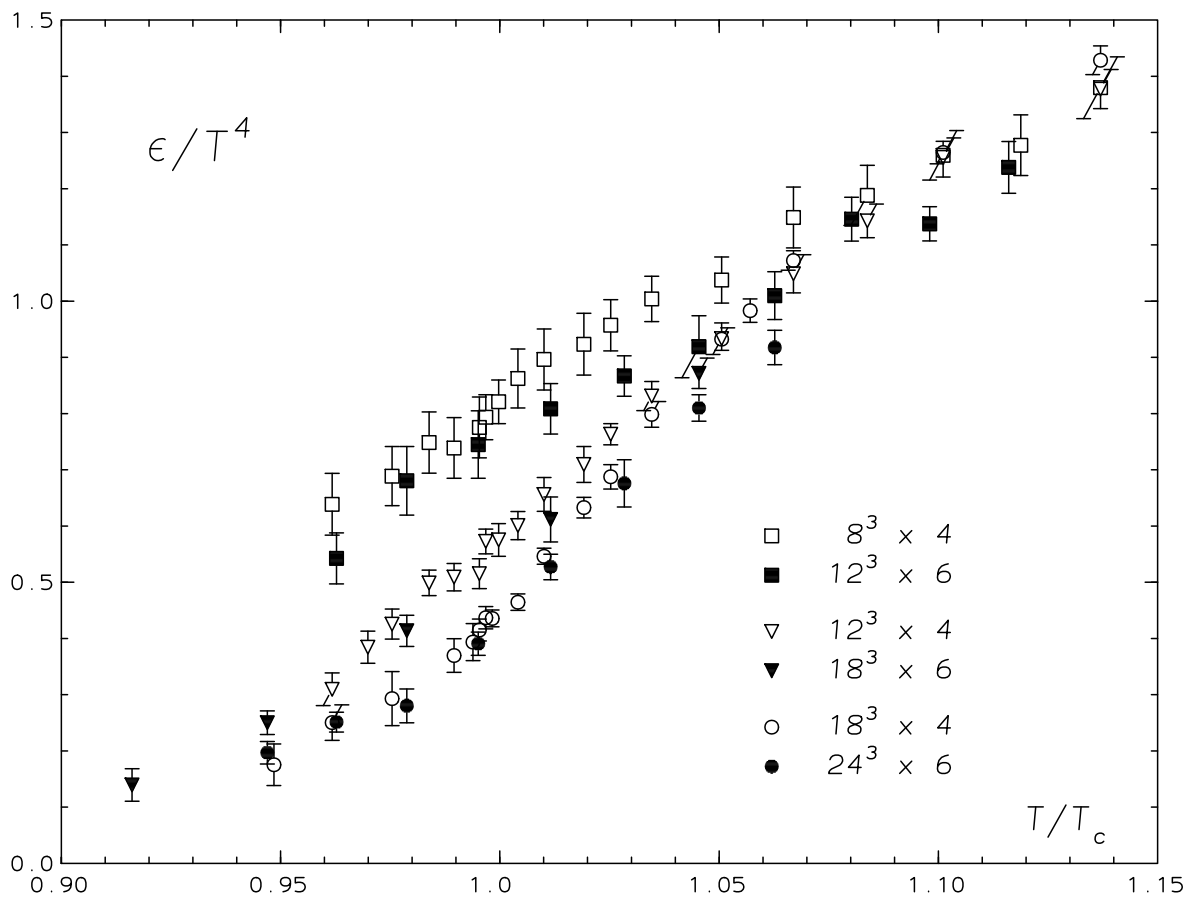


Figure 7

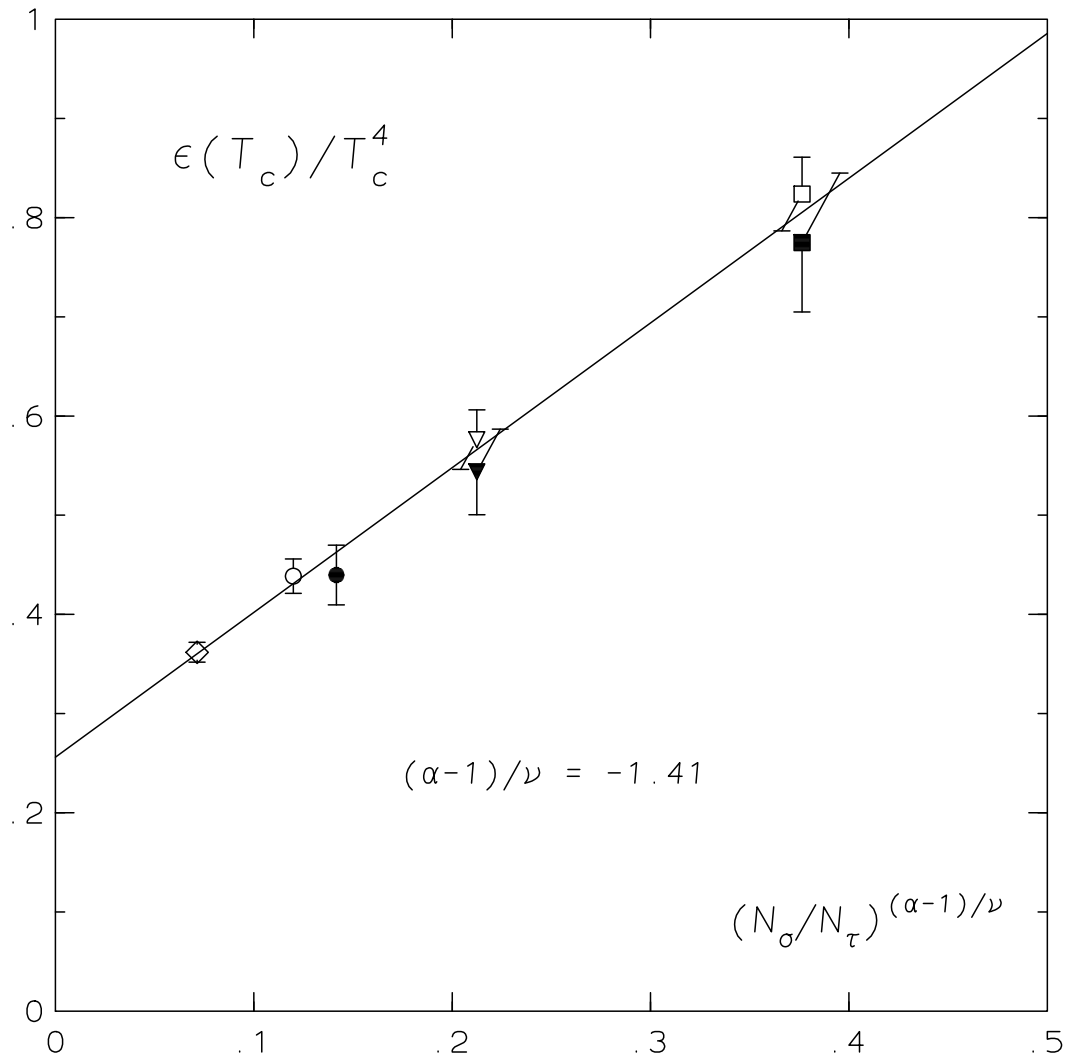


Figure 8



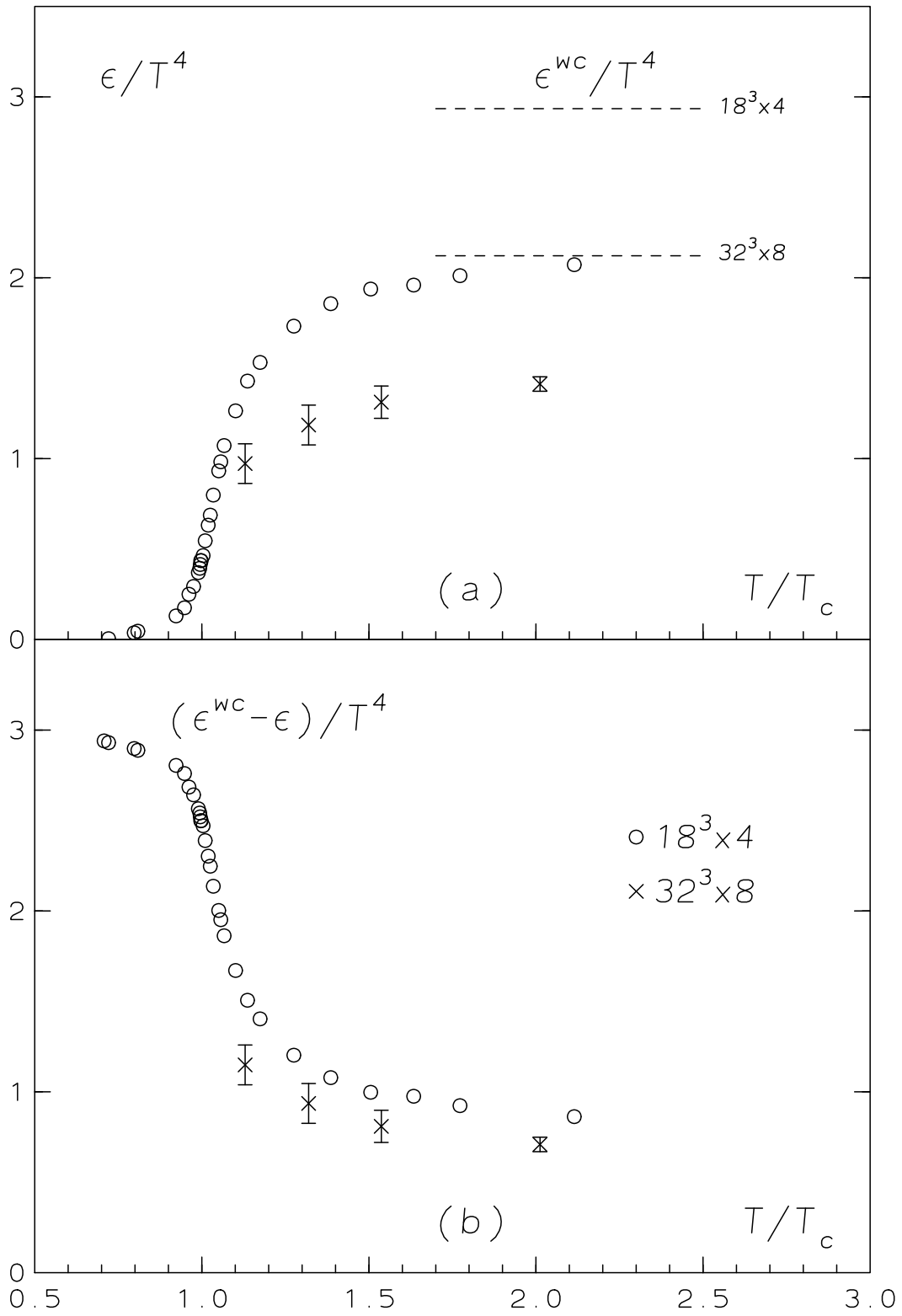


Figure 9